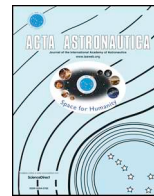




ELSEVIER

Contents lists available at ScienceDirect

Acta Astronautica

journal homepage: [www.elsevier.com/locate/actaastro](http://www.elsevier.com/locate/actaastro)

# Outgassing from the OSIRIS-REx sample return capsule: characterization and mitigation

Scott A. Sandford<sup>a,\*</sup>, Edward B. Bierhaus<sup>b</sup>, Peter Antreasian<sup>c</sup>, Jason Leonard<sup>c</sup>,  
Christopher K. Materese<sup>a,d,e</sup>, Christian W. May<sup>b</sup>, Jarvis T. Songer<sup>b</sup>, Jason P. Dworkin<sup>e</sup>,  
Dante S. Lauretta<sup>f</sup>, Bashar Rizk<sup>f</sup>, the OSIRIS-REx Team<sup>1</sup>

<sup>a</sup> NASA Ames Research Center, Astrophysics Branch, MS 245-6, Moffett Field, CA 94035, USA

<sup>b</sup> Lockheed Martin Space Systems, Littleton, CO, USA

<sup>c</sup> KinetX Aerospace, Space Navigation and Flight Dynamics, Simi Valley, CA, USA

<sup>d</sup> BAER Institute, NASA Research Park, Bldg. 18, Rm. 101, MS 18-4, Moffett Field, CA 94035, USA

<sup>e</sup> NASA Goddard Space Flight Center, Astrochemistry Lab, MS 691, Greenbelt, MD 20771, USA

<sup>f</sup> Lunar and Planetary Laboratory, University of Arizona, Tucson, AZ 85721, USA

## ARTICLE INFO

### Keywords:

OSIRIS-REx  
Bennu  
Asteroid  
Sample return  
Outgassing

## ABSTRACT

The Origins, Spectral Interpretation, Resource Identification, and Security–Regolith Explorer (OSIRIS-REx) spacecraft launched on September 8, 2016, beginning a seven-year journey to return at least 60 g of asteroid material from (101955) Bennu to Earth. During the outbound cruise, Doppler tracking of the spacecraft observed a small but measurable acceleration when the sample return capsule (SRC) was first placed in sunlight. Subsequent analysis determined that outgassing from the SRC is the most likely cause for the acceleration. This outgassing received combined engineering and scientific attention because it has potential implications both for spacecraft navigation performance and for contamination of the collected samples. Thermal modeling, laboratory studies of SRC materials, and monitoring of the acceleration are all consistent with H<sub>2</sub>O as the main component of the outgassing. Dedicated, in-flight campaigns continued to expose the SRC to sunlight until the acceleration dropped to the acceleration noise floor. Any residual amounts of H<sub>2</sub>O outgassing are not considered to be a hazard with regards to mission operations or pristine sample acquisition. The sample stow procedure has been updated to ensure that no direct line of site exists between any residual outgassing and the samples during future operations. Similar outgassing of the Stardust SRC probably also occurred. No adverse contamination of Stardust samples was observed that could be associated with this process. Future missions that use similar reentry vehicles should consider procedures to test for and, if necessary, mediate such outgassing after launch.

## 1. Introduction

### 1.1. Mission overview

The Origins, Spectral Interpretation, Resource Identification, and Security–Regolith Explorer (OSIRIS-REx) asteroid sample return mission is NASA's third mission in the New Frontiers program. The primary objective of OSIRIS-REx is to survey near-Earth asteroid (101955) Bennu and return a sample of its regolith to Earth so that we can study its physical, mineralogical, and chemical properties; assess its resource potential; and

refine our understanding of it as an impact hazard [1]. Bennu has a very low albedo and is a spectral B-type asteroid likely related to carbonaceous chondrites [2–5], meteorites that record the history of volatiles and organic compounds in the early Solar System. Bennu is so small (500 m diameter) that the solar pressure on the spacecraft is on the same order of magnitude as the gravitational attraction to Bennu. Given the need to precisely control navigation around Bennu [1,6] and to collect and return a sample free of spacecraft outgassing materials [7], a detailed understanding of the outgassing that can exert a thrust on the spacecraft and potentially contaminate the sample is required.

\* Corresponding author. NASA Ames Research Center, Astrophysics Branch, Mail Stop 245-6, Moffett Field, CA 94035, USA.

E-mail addresses: [Scott.A.Sandford@nasa.gov](mailto:Scott.A.Sandford@nasa.gov) (S.A. Sandford), [edward.b.bierhaus@lmco.com](mailto:edward.b.bierhaus@lmco.com) (E.B. Bierhaus), [peter.antreasian@kinetx.com](mailto:peter.antreasian@kinetx.com) (P. Antreasian), [Jason.Leonard@kinetx.com](mailto:Jason.Leonard@kinetx.com) (J. Leonard), [Christopher.K.Materese@nasa.gov](mailto:Christopher.K.Materese@nasa.gov) (C.K. Materese), [christian.w.may@lmco.com](mailto:christian.w.may@lmco.com) (C.W. May), [jarvis.t.songer@lmco.com](mailto:jarvis.t.songer@lmco.com) (J.T. Songer), [Jason.P.Dworkin@nasa.gov](mailto:Jason.P.Dworkin@nasa.gov) (J.P. Dworkin), [lauretta@orex.lpl.arizona.edu](mailto:lauretta@orex.lpl.arizona.edu) (D.S. Lauretta), [bashar@lpl.arizona.edu](mailto:bashar@lpl.arizona.edu) (B. Rizk).

<sup>1</sup> [correspondence@orex.lpl.arizona.edu](mailto:correspondence@orex.lpl.arizona.edu)

<https://doi.org/10.1016/j.actaastro.2019.07.043>

Received 7 February 2019; Received in revised form 24 May 2019; Accepted 15 July 2019

Available online 15 October 2019

0094-5765/ Published by Elsevier Ltd on behalf of IAA.

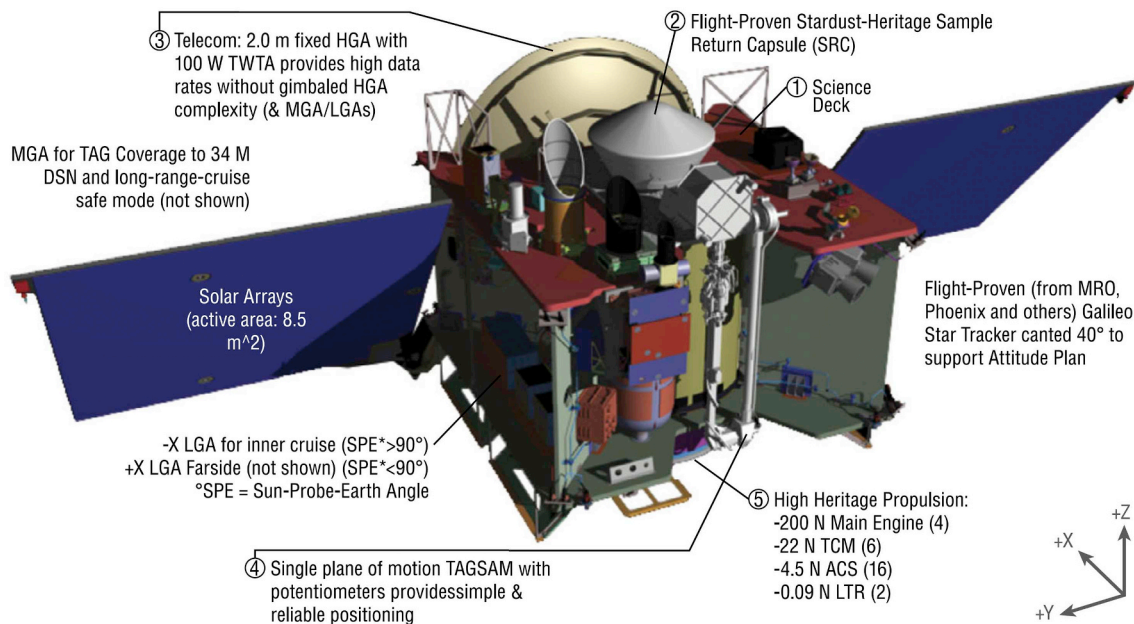


Fig. 1. The OSIRIS-REx spacecraft. The SRC, scientific instruments, and TAGSAM are all mounted on the +z deck at the top of the figure (image from Fig. 9 of [1]).

## 1.2. Overview of the spacecraft and sampling acquisition and return system

OSIRIS-REx was launched on September 8, 2016 and began the approach to Bennu on August 17, 2018. After an extensive survey of the asteroid using a number of onboard instruments, sample collection is scheduled for July 2020. The spacecraft will leave Bennu in 2021 and return the samples to the Utah Test and Training Range (UTTR) on September 24, 2023 [1].

The OSIRIS-REx spacecraft bus contains the spacecraft structure and all supporting subsystems for the operation and control of the vehicle. On the +z deck of the bus (Fig. 1) are the five science instruments responsible for the remote-sensing campaign at Bennu [8–12]. Also on the +z deck is the Sample Acquisition and Return Assembly (SARA) which supports the Touch and Go Sample Acquisition Mechanism (TAGSAM) and the Sample Return Capsule (SRC) [13].

The SRC used by OSIRIS-REx is nearly identical to the one developed by Lockheed Martin for the Stardust comet sample return mission (Fig. 2) [13–15]. Updates to the Stardust SRC design include differences in the ballast, added contamination witness plates, and accommodations for TAGSAM rather than the Stardust aerogel paddle. The OSIRIS-REx heatshield and backshell are made from the same materials used for the Stardust SRC.

The heatshield consists of a graphite-epoxy material covered with a thermal protection system that uses Phenolic-Impregnated Carbon Ablator (PICA), the same material used on the Stardust heatshield. PICA is a lightweight material developed to withstand high temperatures and mechanical stress [17]. The principle behind ablative heat shield technology is to create a boundary layer between the heatshield's outer surface and the extremely hot shock gas generated in and around the capsule during reentry. This boundary layer is created as the shield slowly ablates away, which generates gaseous reaction products that flow out of the shield and keep the shock layer at a separation distance. This configuration reduces the overall heat flux experienced by the outer shell of the capsule. Development and production of the PICA for both the Stardust and OSIRIS-REx missions was carried out by Fiber Materials Inc.

The backshell of the SRC is also covered with thermal protection material, but because it resides in the wake of the hot gas flow, less protection is required. It uses a cork-based material known as SLA 561V, originally developed by Lockheed Martin for the Viking missions to Mars in the 1970s and since used on many missions, including the Mars Landers Phoenix and InSight.

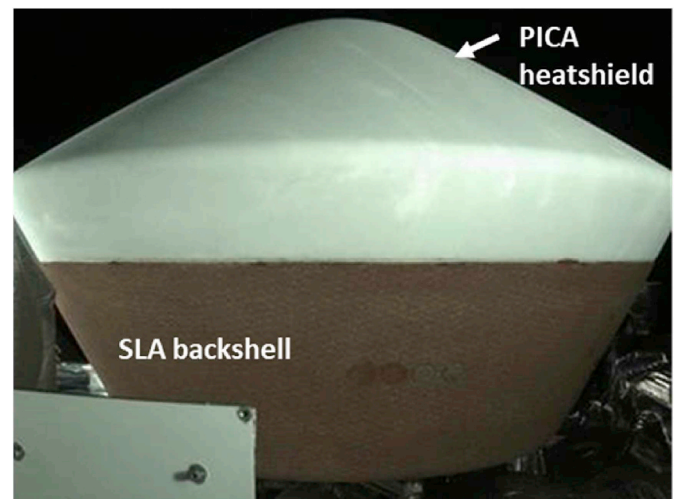


Fig. 2. The OSIRIS-REx SRC. The white upper component is the PICA heatshield. The tan lower component is the SLA backshell. StowCam acquired this image after launch. StowCam monitors the insertion of the collected sample into the SRC [13,16].

## 2. Detection, monitoring, and mitigation of outgassing

The acceleration due to SRC outgassing was not anticipated prior to launch. The following describes the conditions that led to the initial outgassing detection, and the steps taken to monitor and mitigate the outgassing.

### 2.1. Initial detection

During the outbound cruise phase between launch and approach to Bennu, the operations team placed the spacecraft in specific attitudes that correspond to events across the mission duration. The purpose of these activities is to test the spacecraft response as a means to prepare for the actual events later in the mission. One such test event, called an SRC “toe dip” event, was an opportunity to test the thermal response of the spacecraft to a specific attitude and solar range that corresponds to what the SRC will encounter at Earth return in September 2023. The

spacecraft initiated the SRC toe dip event on February 22, 2017 and maintained the attitude for more than 21 h (75000 s). The OSIRIS-REX navigation team noted an unexpected acceleration in the  $-z$  spacecraft direction, coincident with the entire duration of the SRC toe dip. This event was the first extended exposure of the SRC to the Sun since the launch of the spacecraft. The magnitude of the acceleration was about two orders of magnitude larger than the minimum observable acceleration (i.e., the acceleration noise floor), and about one order of magnitude larger than accelerations due to solar radiation pressure on the spacecraft.

The prime candidate for the source of the acceleration was outgassing from the SRC. The correlation between the onset of the acceleration and the exposure of the SRC to the Sun, and the direction of the acceleration ( $\sim 180^\circ$  from the orientation of the SRC), made outgassing an early, and testable hypothesis. Outgassing raised several potential concerns for the mission, the severity of which depends on both the amount of material outgassed and its composition. These concerns include:

- (1) Potentially unpredictable trajectory perturbations during proximity operations at Bennu, when our knowledge of and capability to predict the spacecraft's position are very sensitive to small accelerations
- (2) Potential contamination of the collected sample (particularly problematic if the outgassing material is organic)

Sources of water ice were known to exist on the spacecraft, but were expected to be depleted, and originally would not contain enough water to cause the repeated and prolonged accelerations observed during the toe-dip attitude. Rizk et al. [18] observed bright streaks in images acquired during the OSIRIS-REx Earth Trojan survey; they propose the most likely explanation for the streaks is a population of water-ice particles released from the spacecraft deck. That portion of the deck had been shaded and cold during cruise, and was warmed to higher-rate, water-ice sublimation temperatures for the first time during the survey. The outgassing described here, also thought to be primarily water, is sourced from the SRC and likely was released entirely in the gas phase. The presence of residual water ice on the spacecraft is not surprising; indeed spacecraft outgassing is a well-known phenomenon, in some cases well characterized by onboard mass spectrometers (e.g. Ref. [19]).

## 2.2. Monitoring and mitigation

As a result of the first two unexpected acceleration events, and because outgassing was the suspected root cause, the OSIRIS-REx operations and navigation teams planned a campaign of repeated in-flight activities that placed the SRC in sunlight for extended periods.

This campaign occurred between October 2017 and March 2018 when the spacecraft attitude periodically tilted the SRC towards the Sun. The tilt varied from  $20^\circ$  to  $45^\circ$ ; higher angles exposed more of the SRC to sunlight. Fig. 3 plots the modeled accelerations, derived from Doppler tracking data between the spacecraft and the NASA Deep Space Network, from the initial outgassing observations through the final outgassing event. Each outgassing maneuver occurred at different solar ranges and with different spacecraft attitudes relative to Earth (which affects the observed Doppler signal). Although these factors introduce variability into the modeled acceleration, the outgassing events include different solar ranges for a given spacecraft attitude, providing data to solve for the two effects independently. The overall trend for the accelerations is a definitive decrease, and the modeled acceleration from the last outgassing attitude is below the minimum observable acceleration, demonstrating that the effect reached an unmeasurable, and thus safe, level for proximity operations around Bennu. Unmodeled accelerations at this level do not impact operations.

## 3. Outgassing evaluation

### 3.1. Spacecraft operations team evaluation

During nominal cruise activities, the spacecraft's high-gain antenna shades the SRC from the Sun. In this geometry, temperatures for the heatshield are  $\geq 170$  K, and temperatures for the backshell are  $\geq 200$  K. This attitude has been in place for the majority of the outbound cruise, except for occasional excursions to other attitudes, such as the Earth-Trojan search [1]. In those other attitudes, the SRC either remained shaded or was exposed to the Sun for very short times. For the SRC toe dip attitude, the SRC was tilted  $45^\circ$  towards the Sun, which put the heatshield, and a small portion of the backshell, in direct sunlight for an extended period—the first such extended exposure since launch. Fig. 4 illustrates the nominal cruise and SRC toe dip attitudes.

The extended exposure of the SRC to sunlight increases the temperature of both the heatshield and the backshell; the outgassing from the SRC could be from one or both items. Initial candidate outgassing materials included adsorbed atmospheric  $H_2O$  and silicone from the SRC coatings. Because outgassing rates depend on temperature, thermal modeling of the SRC provided a basis for constraining which materials could be outgassing during the toe dip. Fig. 5 illustrates the predicted heatshield and backshell temperatures during the initial toe dip event. Peak temperatures of the heatshield reached  $\sim 10^\circ C$ , while peak temperatures of the backshell reached  $\sim 100^\circ C$ . The enhanced temperature of the backshell compared to the heatshield is due to several sources, including reduced view factor to space relative to the heatshield (reducing radiative cooling), greater thermal load from the spacecraft top deck, added flux from reflections off the spacecraft top deck, and because the backshell surface color is lower albedo than the heatshield (see Fig. 2).

The thermal modeling demonstrates that the temperatures on both the heatshield and backshell were insufficient to induce silicone outgassing, yet were more than sufficient to cause outgassing of  $H_2O$ . Fig. 6 plots the sublimation rate of pure  $H_2O$  ice in a vacuum, following the methodology of Andreas [20]. The plot demonstrates the strong sensitivity of the sublimation rate to temperature. Increases of only a few degrees substantially increase the sublimation rate by factors of  $\sim 2$ – $10$ , depending on the starting temperature [21]. Though sublimation from pure  $H_2O$  ice is not directly analogous to sublimation from the SRC, the behavior of pure  $H_2O$  ice at room temperature (the temperature range experienced by portions of the heatshield) demonstrates the well-known mobility of the material in vacuum, and  $H_2O$  ice must be even more mobile at higher temperatures (experienced within portions of the backshell).

Given that temperatures were sufficient to cause  $H_2O$  sublimation from the SRC, the next investigative step was to determine whether trapped  $H_2O$  in the SRC could cause the derived acceleration. A simple treatment of this question is to use conservation of momentum. Consider a reference frame in which the spacecraft is at rest pre-outgassing. After the outgassing, the spacecraft experiences a momentum change that must be equivalent to the momentum carried by the sublimated  $H_2O$ . This is expressed as

$$m_{sc} v_{sc} = m_w v_w \quad (1)$$

where  $m_{sc}$  and  $v_{sc}$  are the mass and velocity of the spacecraft, respectively, and  $m_w$  and  $v_w$  are the mass and velocity of the sublimated  $H_2O$ .

The mass and velocity of the spacecraft after outgassing are reasonably well constrained, whereas the mass and velocity of any sublimated  $H_2O$  are not. The amount of  $H_2O$  resident in the heatshield could be 100 g to nearly 400 g. The amount of  $H_2O$  in the backshell is also uncertain, but because of the much lower mass of backshell material, the backshell would contribute at most only tens of grams of additional water. To estimate the water velocity, we assumed a theoretical maximum limit velocity for the sublimating gas, with

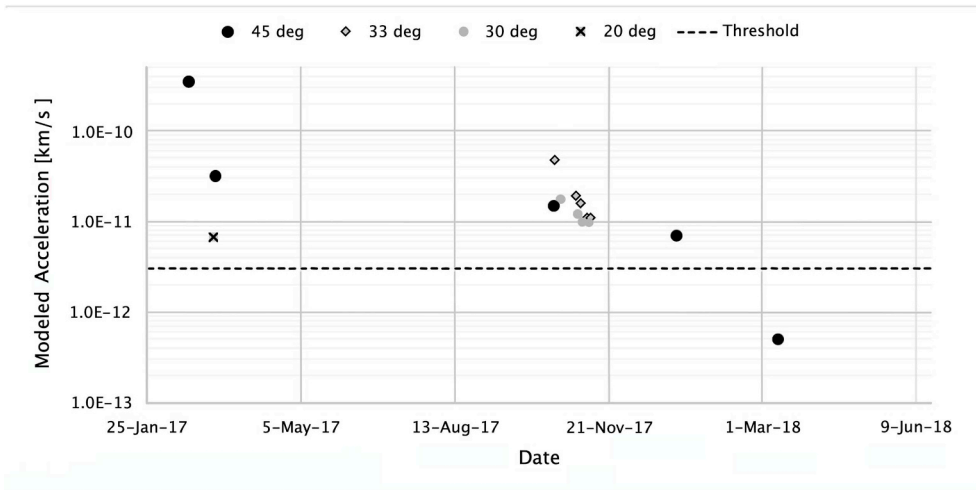


Fig. 3. The discrete data points are modeled accelerations due to outgassing. The different symbols correspond to different sun-point attitudes of the spacecraft. The dashed black line is approximately the minimum observable acceleration. The data point at the earliest calendar date shows the first observation of outgassing, followed by two additional data points in March 2017 that confirmed the initial detection. Subsequent dedicated outgassing campaigns continued to deplete the outgassing effects, and the modeled acceleration from the final outgassing event was below the minimum detectable threshold, indicating that the effect had reached an unmeasurable, and thus safe, level.

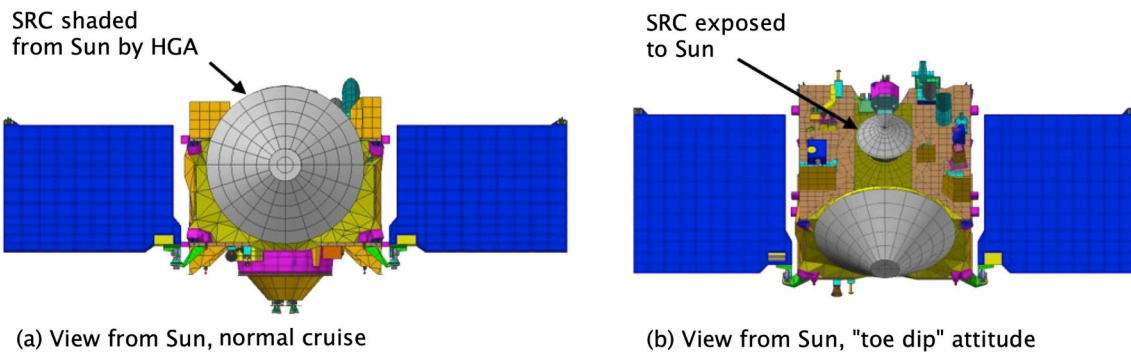


Fig. 4. (a) The spacecraft seen from the Sun vector during the nominal cruise attitude. In this attitude the SRC is shaded by the spacecraft's high-gain antenna (HGA). (b) The spacecraft as seen from the Sun vector during the SRC toe dip, which exposes the heatshield and part of the backshell to the Sun.

$$v_w = v_{limit} = \left( \frac{2\gamma RT_0}{\gamma - 1} \right)^{\frac{1}{2}} \quad (2)$$

where  $\gamma$  is the ratio of specific heats,  $R$  is the specific gas constant, and  $T_0$  is the total temperature at zero velocity. For  $\gamma = 1.33$ , and  $R = 461.5 \text{ J kg}^{-1} \text{ K}^{-1}$ , Fig. 7 plots the exit velocity of a water molecule from the warmer portion of the SRC. A typical value is  $\sim 1000 \text{ m/s}$ .

The derived acceleration from the outgassing event corresponds to a

total velocity change ( $\Delta v$ ) to the spacecraft of  $\sim 1.4 \times 10^{-5} \text{ m/s}$ .  $\text{H}_2\text{O}$  trapped in the SRC must be sufficient to supply this velocity change to the spacecraft, as well as the additional velocity changes during the subsequent outgassing campaign. Using conservation of momentum, the estimated  $\Delta v$  to the spacecraft from the sublimating  $\text{H}_2\text{O}$  is

$$\Delta v_{sc} = \frac{v_w * m_w}{m_{sc}} \quad (3)$$

Fig. 8 plots the theoretical maximum  $\Delta v$  that water stored in the SRC

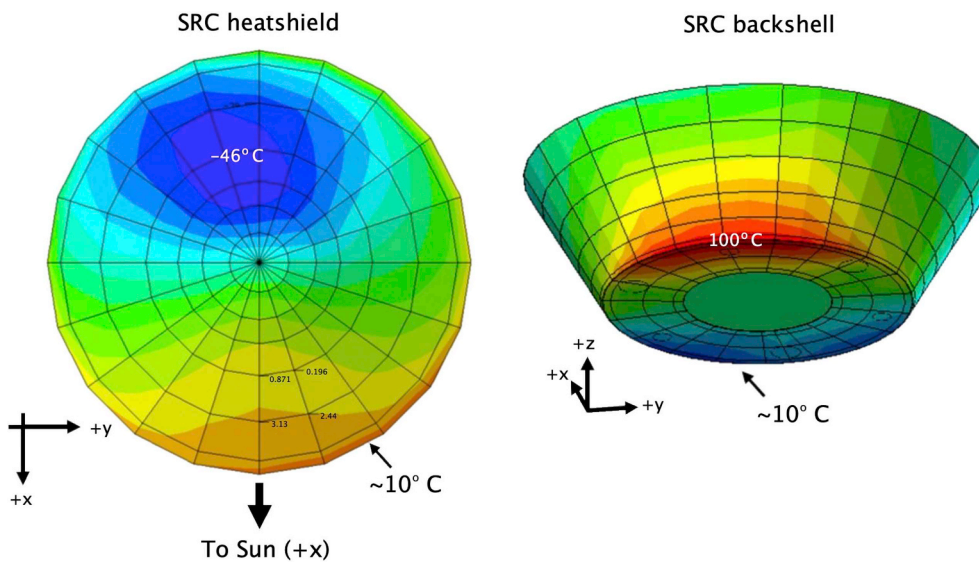


Fig. 5. Expected temperatures for the SRC heatshield (left) and backshell (right) at the initial SRC toe dip attitude on February 22, 2017. In both views,  $+x$  is towards the Sun. (In the right-hand view, the  $+x$  axis points out from the page and slightly up.) During the nominal cruise attitude, the  $+z$  axis is perpendicular to the Sun, and is shaded by the spacecraft's high-gain antenna; during the toe dip attitude, the  $+z$  axis is tipped  $45^\circ$  towards the Sun, directly illuminating part of the SRC and backshell (Fig. 4).

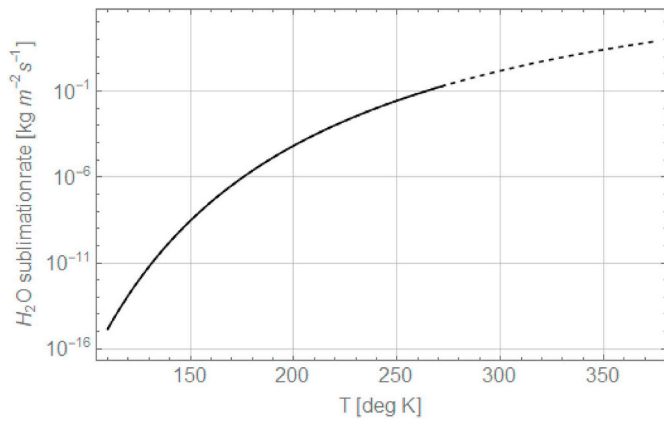


Fig. 6. The sublimation rate of pure water ice, in vacuum, using the methodology summarized in Andreas [20]. The solid line is for the temperature range of the published fit [110 K–273 K]; the dashed line is an extrapolation of that function to the predicted maximum SRC temperatures during the toe dip.

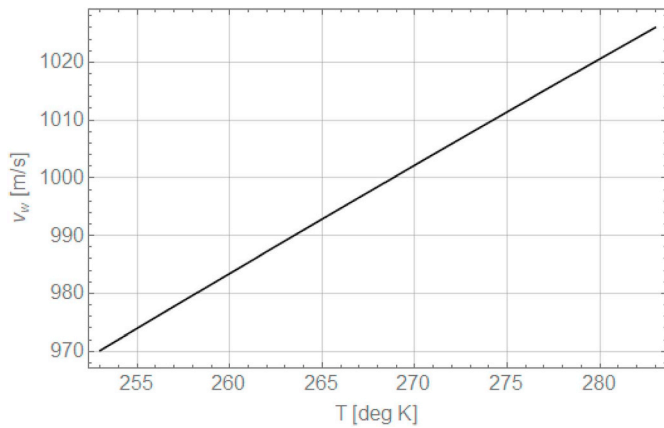


Fig. 7. The idealized exit velocity of sublimating H<sub>2</sub>O molecules over the predicted surface temperature range of the warmer portion of the heatshield.

could generate by outgassing, assuming  $v_w = 1000$  m/s,  $m_{sc} = 1743$  kg, and that  $m_w$  could vary from 0.1 to 0.4 kg. Even at 100 g of water, the total idealized  $\Delta v$  is several orders of magnitude above the estimated  $\Delta v$  from the toe dip attitude and the subsequent outgassing activities. The actual  $\Delta v$  will be less than the idealized amount because (i) the

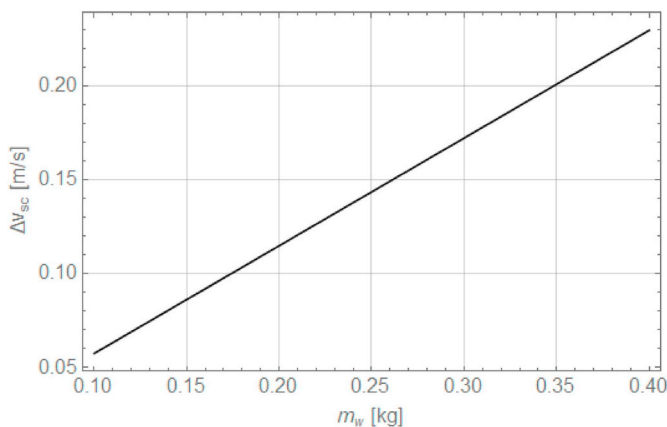


Fig. 8. The idealized, total possible change in spacecraft velocity ( $\Delta v_{sc}$ ) due to H<sub>2</sub>O outgassing, as a function of the mass of H<sub>2</sub>O ( $m_w$ ) stored in the SRC. The total possible  $\Delta v$  exceeds the observed  $\Delta v$ , demonstrating that H<sub>2</sub>O outgassing from the SRC is a viable explanation for the unexpected acceleration during the toe dip campaign.

estimated sublimation velocity of the H<sub>2</sub>O molecules is a theoretical maximum, and (ii) although the net acceleration was primarily in the  $-z$  direction, not all H<sub>2</sub>O molecules left the SRC surface in the  $+z$  direction. Accounting for these factors reduces the  $\Delta v$  capacity of outgassing H<sub>2</sub>O by up to a factor of two, but that still is a sufficient amount to cause the observed trajectory perturbations. Thus, H<sub>2</sub>O stored in the SRC was a viable reservoir of outgassing material that could have affected the spacecraft as observed.

Because the SRC temperatures during the toe dip were too low to cause silicone outgassing, and because of the absence of another reservoir of material to outgas, the spacecraft team concluded that the outgassing of H<sub>2</sub>O from the SRC was the most likely explanation for the unexpected acceleration.

### 3.2. Laboratory tests to constrain the outgassed materials

We examined the potential scientific implications of the outgassing in parallel with the spacecraft team's evaluation described in the previous section. Members of the science team carried out laboratory tests of sample heatshield and backshell materials to search for and characterize outgassing products released when these materials are warmed. In particular, a series of laboratory heating experiments were carried out on samples of both materials in the Astrochemistry Laboratory at NASA's Ames Research Center.

Three types of samples were studied:

Sample type #1 - OSIRIS-REx PICA. Individual samples were  $\sim 1.5$  cm  $\times$  1.5 cm  $\times$  5 cm in dimension and had a visible layer of clearcoat/paint on one of the  $\sim 1.5$  cm  $\times$  1.5 cm faces.

Sample type #2 - InSight SLA. Individual samples were 1.5 cm  $\times$  1.5 cm  $\times$  2 cm and had an aluminum plate on one of the 1.5 cm  $\times$  1.5 cm faces.

Sample type #3 - OSIRIS-REx SLA. Individual samples were  $\sim 1.5$  cm  $\times$  1.5 cm  $\times$  1 cm and had an aluminum plate on one of the 1.5 cm  $\times$  1.5 cm faces. Infrared reflection spectra taken from the side opposite the aluminum plate confirmed the presence of clearcoat on that surface.

We used a Bio Rad Excalibur Fourier-transform infrared (FTIR) spectrometer to obtain 6000 to 600  $\text{cm}^{-1}$  infrared reflection spectra at a spectral resolution of 1  $\text{cm}^{-1}$  from the original surfaces of all three sample types. In the case of the OSIRIS-REx samples, we obtained spectra from both coated and uncoated surfaces. We also obtained similar infrared spectra from these types of samples after heating to 110 °C. We took all of these spectra (both pre- and post-heating) for comparison with the infrared spectra of gases released during sample heating.

#### 3.2.1. Testing for the release of volatile gases

We tested each of the sample types for their release of volatile gases at temperatures of 50 °C and 110 °C. We did this by placing full blocks of each sample type into a test chamber, evacuating the chamber of air, heating the chamber, and collecting any released gases. The basic steps of the procedure for each material were as follows:

- (1) Samples (an entire block of PICA, or three blocks of each of the SLAs) were placed in a small aluminum test chamber and the chamber was sealed.
- (2) The chamber, which was connected to a vacuum glass line, was then pumped out at room temperature overnight. The samples all released gases during this period, but the rate of release dropped steadily with time. By the next morning the glass line was usually at the lower limit of its normal evacuated pressure ( $1 \times 10^{-6}$  mbar), although closing and later opening of the valve that isolated the test chamber from the glass line made it clear that the materials in the test chamber were still outgassing slowly, even at room temperature.

- (3) The test chamber was next isolated from the glass line vacuum system and connected to a pre-evacuated 2-L glass bulb cooled by LN<sub>2</sub>.
- (4) Heat tape was then used to heat the chamber to 50 °C. This process typically took 15 min. Once the chamber reached 50 °C it was maintained at that temperature for 2 h. Released gases were collected in the glass bulb during the entire heating period. During this period, the bulbs should have collected nearly 100% of any released gases that condense at the temperature of LN<sub>2</sub> (for example, H<sub>2</sub>O and CO<sub>2</sub>). In addition, because the bulbs represent ≥90% of the volume of the system in the collection configuration, they should also have collected ≥90% of any non-condensable gases present (for example, O<sub>2</sub>, N<sub>2</sub>, CO, etc.).
- (5) At the end of 2 h, we sealed the sample chamber and we sealed and removed the glass sample bulb. We then replaced this bulb with a new, pre-evacuated glass sample bulb, also cooled by LN<sub>2</sub>.
- (6) We re-opened the test chamber valve, opened the valve on the new bulb, and turned up the power on the heat tape to heat the chamber to 110 °C. This process typically took 25 min. Once the chamber reached 110 °C, it was maintained at that temperature for 1 h. Released gases collected in the second glass bulb during the entire heating period.
- (7) At the end of 1 h at 110 °C, we sealed the chamber and glass sample bulb and removed the glass bulb. The chamber was allowed to cool to room temperature.
- (8) We removed the heated samples from the test chamber and stored them separately from the original unheated samples. No visible change was caused by the heating in any of the samples.
- (9) We subsequently mounted the glass sample bulbs with their captured gases on a cryo-vacuum system whose sample chamber was placed in the beam of an FTIR spectrometer.
- (10) We measured the pressures in each of the bulbs at this time. They were:

OSIRIS-REX PICA (sample type #1), 50 °C, pressure = 3.2 mbar.

OSIRIS-REX PICA (sample type #1), 110 °C, pressure = 7.9 mbar.

InSight SLA (sample type #2), 50 °C, pressure = 4.7 mbar.

InSight SLA (sample type #2), 110 °C, pressure = 15.4 mbar.

OSIRIS-REX SLA (sample type #3), 50 °C, pressure = 2.1 mbar.

OSIRIS-REX SLA (sample type #3), 110 °C, pressure = 8.8 mbar.

All samples released more gas in 1 h at 110 °C than in 2 h at 50 °C.

Also, the SLA samples released more gas per volume of material than the PICA by roughly a factor of 4 (discussed in more detail in section 3.2.1.3).

- (11) We cooled the sample window at the end of the cryostat to ~25 K, and a portion of the gases in each bulb was condensed onto the window so we could obtain their infrared spectra.

**3.2.1.1. OSIRIS-REX PICA (sample type #1).** The infrared spectra of the gases released from PICA during both the 50 °C and 110 °C heatings are dominated by H<sub>2</sub>O, as demonstrated by the prominent O–H stretching, H–O–H bending, and libration modes at 3260, 1650, and 770 cm<sup>-1</sup>, respectively, and overtone/combination modes at 2435 and 2200 cm<sup>-1</sup> [22,23] (Fig. 9). Gases released at both temperatures also contain a small amount of CO<sub>2</sub>, as evidenced by the fundamental C–O stretching and O–C–O bending mode features near 2335 and 645 cm<sup>-1</sup>, respectively, as well as some weaker overtone and combination modes [24,25]. The lack of any substantial “dangling –OH” features in the H<sub>2</sub>O spectrum in the 3660 to 3710 cm<sup>-1</sup> range indicate that infrared-inactive molecules such as N<sub>2</sub> or O<sub>2</sub> are not abundant in the samples [26] — i.e., the adsorbed gases are not adsorbed air. Many very weak features are evident in the 1700 to 900 cm<sup>-1</sup> region, with more features being apparent in the 110 °C spectrum than in the 50 °C spectrum. An expanded view of this spectral region is shown in Fig. 10 for samples from both the 50 °C and 110 °C heatings.

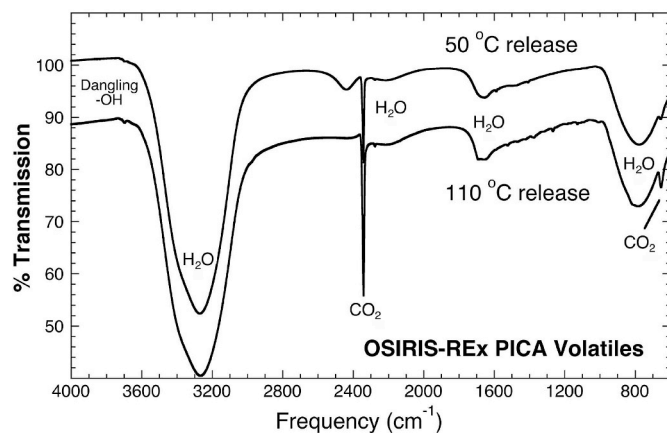


**Fig. 9.** The mid-infrared spectra of gases released from PICA at 50 °C and 110 °C show that the dominant components are H<sub>2</sub>O and CO<sub>2</sub>. The presence of only very weak “dangling –OH” features in the 3660 to 3710 cm<sup>-1</sup> range indicate that N<sub>2</sub> or O<sub>2</sub> are not abundant in the samples and that the gas is not adsorbed air.

**3.2.1.2. InSight and OSIRIS-REX SLA (sample types #2 and #3).** For both the InSight SLA and the OSIRIS-REX SLA, only H<sub>2</sub>O and traces of CO<sub>2</sub> are evident in the 50 °C and 110 °C releases. Fig. 11 shows the infrared spectra of the gases released by the OSIRIS-REX SLA samples. No substantive additional features are apparent in the spectra from any of the SLA samples. Again, the lack of strong dangling –OH features in the 3660 to 3710 cm<sup>-1</sup> range indicate that infrared-inactive molecules such as N<sub>2</sub> or O<sub>2</sub> are not abundant in the gas sample—i.e., the adsorbed gases are not adsorbed air.

**3.2.1.3. Amounts of volatile gases released during 50 °C and 110 °C heatings.** The amount of material released from each heating of the samples can be calculated using the ideal gas law and the measured sample bulb pressures and volumes. The amount of gas released per volume of the PICA and SLA samples can then be determined by dividing the amount of collected gas released by the heatings by the volume of the heated samples. The results are summarized in Table 1. In general, SLA releases ~3.5 times as much gas per cubic centimeter as

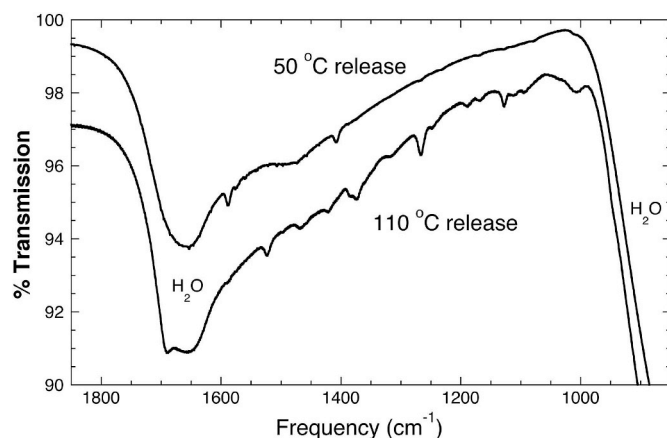


**Fig. 10.** An expanded plot showing the weaker features in both the 50 °C and 110 °C samples in the 1800 to 1000 cm<sup>-1</sup> region. The overall dip in this spectral region is due to the H–O–H bending mode of H<sub>2</sub>O ice. Features are evident in the 50 °C sample at 1588, 1474, and 1406 cm<sup>-1</sup>. These features are also apparent in the 110 °C spectrum, albeit more weakly, and are joined by additional features at 1685, 1523, 1421, 1376, 1315, 1266, 1246, 1187, 1167, 1127, 1109, 1093, and 1005 cm<sup>-1</sup>. These features do not match those from the original PICA or PICA clearcoat (either heated or unheated), and their source(s) are currently unidentified.

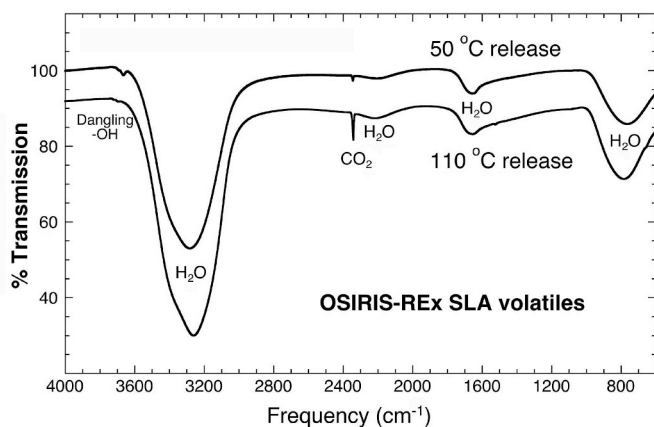


Fig. 11. The mid-infrared spectra of condensed gases released by OSIRIS-REx SLA when heated to 50 °C and 110 °C. The features of H<sub>2</sub>O dominate the spectra. The only other identified molecule present is CO<sub>2</sub>. The spectra of the materials released by the InSight SLA samples show the same features.

PICA at 50 °C and ~5 times as much gas per cubic centimeter as PICA at 110 °C.

These numbers apply only to the gases captured during the 50 °C and 110 °C heatings. Considerable additional gases were released during the overnight room-temperature pump-out that preceded the heating tests. Adsorbed air and H<sub>2</sub>O likely dominated this gas. If the SRC cooled quickly after launch, it might have retained some of these gases and they would have been available for subsequent outgassing as well.

### 3.2.2. Tests for the release of refractory gases that recondense at room temperature

The above tests are only informative for released gases that remain in the gas phase at room temperature. To look for possible refractory gases released at 110 °C that recondense at room temperature, we heated samples in the presence of aluminum foil used as witness plates on which outgassing material could condense. We only carried out these tests for material associated with the clear coated surface layers of sample types #1 and #3. The steps for executing these tests were as follows:

- (1) The surface layers associated with clear-coat were cut away from the ends of a block of OSIRIS-REx PICA (sample type #1) and OSIRIS-REx SLA (sample type #3) using a clean razor blade. The covering layer on the PICA was easily seen, but there was no visible evidence of a layer on the OSIRIS-REx SLA. However, the presence of a coating on the SLA was confirmed using infrared reflection spectroscopy.
- (2) The two samples were each placed in a glass sample tube that could be vacuum-sealed with a Teflon stopcock.
- (3) A rolled cylinder of pre-baked aluminum foil was dropped into each tube with the samples.
- (4) The glass sample tubes were both evacuated of air and sealed.
- (5) The glass sample tubes were placed in an oven heated to 110 °C for 1 h before the oven was turned off and the samples allowed to cool.

Table 1

Amounts of gas released during 50 °C and 110 °C heatings.

Sample	Heating temperature (°C)	Released gas (molecules per cubic centimeter of sample) <sup>a</sup>
OSIRIS-REx PICA (sample type #1)	50	$1.5 \times 10^{19}$
OSIRIS-REx PICA (sample type #1)	110	$3.7 \times 10^{19}$
InSight SLA (sample type #2)	50	$5.5 \times 10^{19}$
InSight SLA (sample type #2)	110	$1.8 \times 10^{20}$
OSIRIS-REx SLA (sample type #3)	50	$4.9 \times 10^{19}$
OSIRIS-REx SLA (sample type #3)	110	$2.1 \times 10^{20}$

<sup>a</sup> In all cases “molecules” can be taken to be largely synonymous with “molecules of H<sub>2</sub>O.”

- (6) Once they cooled to room temperature, the sample tubes were removed from the oven and opened so the aluminum foil witness plates could be removed.
- (7) Infrared spectra were obtained from the surfaces of the aluminum foil witness plates and ratioed to background spectra of a bare aluminum foil standard.

No infrared spectral features were seen on the aluminum foil witness plates—i.e., there was no evidence for the presence of any materials that were released at 110 °C from the clearcoat and underlying material that subsequently recondensed onto the aluminum foil witness plates at room temperature.

### 3.2.3. Summary of laboratory test results

The OSIRIS-REx SLA releases only H<sub>2</sub>O and traces of CO<sub>2</sub> when heated to both 50 °C and 110 °C. There is no indication that organics or other more complex molecular species are released during heating to these temperatures. In addition, there is no evidence that heating to 110 °C releases any refractory materials from SLA or the clearcoat on the SLA that would be expected to be re-deposited on room-temperature surfaces. Thus, the outgassing of SLA does not appear to constitute a concern with regards to contamination of Bennu samples.

As with the SLA, the primary material outgassed from heated samples of PICA is H<sub>2</sub>O, followed by smaller amounts of CO<sub>2</sub>. PICA releases small amounts of additional, currently unidentified material(s), possibly organics. These materials are mostly released at 110 °C although even smaller amounts of material are released at 50 °C. Fortunately, whatever these materials are, they are both of low abundance and sufficiently volatile to remain in the gas phase at room temperature—i.e., these are contaminants that would not be expected to linger on surfaces at room temperature.

The full histories of the tested samples are not well established. This ambiguity raises the possibility that these additional materials could be, at least in part, contaminants picked up since manufacture during the past handling or storage of these non-flight samples and that a portion of these contaminants may not be present in the actual flight materials. In this respect, provided there is no heterogeneity between the non-flight and flight materials, the materials measured in our samples may represent an upper limit to what should be on the SRC. However, in the absence of actual flight materials, this is not guaranteed.

The combined heatings to 50 and 110 °C released  $5.2 \times 10^{19}$  molecules per cubic centimeter from OSIRIS-REx PICA and  $2.6 \times 10^{20}$  molecules per cubic centimeter from OSIRIS-REx SLA; that is, the SLA releases 5 times as much gas per cubic centimeter as does the PICA. Again, this gas is almost entirely H<sub>2</sub>O in both cases. As noted earlier, these amounts do not include gases lost during the overnight room temperature pump-out that preceded the heating tests.

These results suggest that we do not need to be concerned about sample contamination associated with outgassing during any maneuvers that heat the SRC to 110 °C. However, it would be best if TAGSAM were not exposed during such outgassing events if it substantially cooler than room temperature, because this opens the possibility of temporary re-condensation of released gases.

#### 4. Comparisons with the Stardust sample return capsule

The materials thought to be responsible for the outgassing measured from the OSIRIS-REx SRC are the same ones used in the Stardust SRC. The Stardust spacecraft did not have constraints that limited the SRC exposure to the Sun. On OSIRIS-REx, because the instruments share the same + z spacecraft deck with the SRC, and because of thermal/solar keep-out zones for the instruments, we could not expose the SRC to full sunlight. Instead, we tilted the +z spacecraft deck towards the Sun at an angle that exposed much of the SRC heatshield to sunlight, while preserving the safety constraints on the instruments. Thus, the Stardust SRC likely also outgassed similar materials during its flight to Comet 81P/Wild 2. Unlike OSIRIS-REx, the Stardust SRC experienced direct solar exposure in its nominal cruise attitude, so likely experienced outgassing early in the mission in the initial days to weeks after launch. In addition, the Stardust spacecraft used uncoupled thrusters for attitude control, so the minimum threshold for unmodeled accelerations was much higher than for OSIRIS-REx, meaning outgassing may not have been visible in the Doppler data.

During its cruise phase, the images provided by the Stardust optical navigation camera degraded in a manner that suggested that some portion of the optics became coated with a condensate. The degradation was later removed when the camera was allowed to warm, suggesting that the deposited material was relatively volatile and not inconsistent with H<sub>2</sub>O. The source of this material was thought to be outgassing from a temporarily trapped atmosphere in the spacecraft after launch. Though there was no direct line of sight between the Stardust SRC and the navigation camera, it is possible that some of the condensates were sourced from water released by the SRC.

Reassuringly, if the Stardust SRC did undergo similar outgassing, it had no observable effects on the samples returned from Comet 81P/Wild 2. An extensive contamination control and assessment study of the samples returned by the Stardust SRC identified no detrimental effects on the samples that were associated with it or any of its components [27].

#### 5. Conclusions

During the OSIRIS-REx spacecraft's outbound cruise, Doppler tracking measured a small acceleration when sunlight illuminated its sample return capsule (SRC). The behavior of the acceleration suggested that outgassing from the SRC was the most likely cause. This outgassing was of concern because it could cause unpredictable trajectory perturbations during proximity operations at Benu and because the outgassing materials could contaminate the samples collected from Benu. Thermal modeling, laboratory studies of SRC materials, and monitoring of the acceleration on the spacecraft are all consistent with the outgassing of H<sub>2</sub>O from the SRC as the primary cause of the accelerations. The outgassing likely comes from both the SRC heatshield and backshell.

In-flight campaigns exposed the SRC to sunlight until the acceleration dropped to the acceleration noise floor. At this point, any residual amounts of H<sub>2</sub>O outgassing are not considered to present a risk in terms of mission operations or sample contamination. As an additional precaution, the sample stow procedure was updated to ensure that no direct line of sight will exist between any residual outgassing and the samples acquired at Benu.

Similar outgassing of the Stardust SRC probably occurred during that mission; no adverse contamination associated with this process was observed on Stardust samples. Future and current missions that use similar reentry vehicles should consider procedures to test for and mediate outgassing after launch.

#### Acknowledgements

We thank the many people whose hard work, dedication, and passion for this mission transformed an idea into a spacecraft at Benu. This work

was supported by the National Aeronautics and Space Administration contracts NNM10AA11C, NNG12FD66C, and NNG13FC02C, and task order NNH09ZDA0070.

#### References

- [1] D.S. Lauretta, S.S. Balram-Knutson, E. Beshore, W.V. Boynton, C. Drouet d'Aubigny, D.N. DellaGiustina, H.L. Enos, D.R. Golish, C.W. Hergenrother, E.S. Howell, C.A. Bennett, E.T. Morton, M.C. Nolan, B. Rizk, H.L. Roper, A.E. Bartels, B.J. Bos, J.P. Dworkin, D.E. Highsmith, D.A. Lorenz, L.F. Lim, R. Mink, M.C. Moreau, J.A. Nuth, D.C. Reuter, A.A. Simon, E.B. Bierhaus, B.H. Bryan, R. Ballouz, O.S. Barnouin, R.P. Binzel, W.F. Bottke, V.E. Hamilton, K.J. Walsh, S.R. Chesley, P.R. Christensen, B.E. Clark, H.C. Connolly, M.K. Crombie, M.G. Daly, J.P. Emery, T.J. McCoy, J.W. McMahon, D.J. Scheeres, S. Messenger, K. Nakamura-Messenger, K. Righter, S.A. Sandford, OSIRIS-REx: sample return from asteroid (101955) Benu, *Space Sci. Rev.* 212 (2017) 925–984.
- [2] B.E. Clark, R.P. Binzel, E.S. Howell, E.A. Cloutis, M. Ockert-Bell, P. Christensen, M.A. Barucci, F. DeMeo, D.S. Lauretta, H. Connolly, A. Soderberg, C. Hergenrother, L. Lim, J. Emery, M. Mueller, Asteroid (101955) 1999 RQ36: spectroscopy from 0.4 to 2.4  $\mu$ m and meteorite analogs, *Icarus* 216 (2011) 462–475.
- [3] C.W. Hergenrother, M.C. Nolan, R.P. Binzel, E.A. Cloutis, M.A. Barucci, P. Michel, D.J. Scheeres, et al., Light curve, color and phase function photometry of the OSIRIS-REx target asteroid (101955) Benu, *Icarus* 226 (2013) 663–670.
- [4] J.P. Emery, Y.R. Fernández, M.S.P. Kelley, K.T. Warden, C. Hergenrother, D.S. Lauretta, M.J. Drake, H. Campins, J. Ziffer, Thermal infrared observations and thermophysical characterization of OSIRIS-REx target asteroid (101955) Benu, *Icarus* 234 (2014) 17–35.
- [5] D.S. Lauretta, A.E. Bartels, M.A. Barucci, E.B. Bierhaus, R.P. Binzel, W.F. Bottke, H. Campins, et al., The OSIRIS-REx target asteroid (101955) Benu: constraints on its physical, geological, and dynamical nature from astronomical observations, *Meteorit. Planet. Sci.* 50 (2015) 834–849.
- [6] B. Williams, P. Antreasian, E. Carranza, C. Jackman, J. Leonard, D. Nelson, B. Page, et al., OSIRIS-REx flight dynamics and navigation design, *Space Sci. Rev.* 214 (2018) 69.
- [7] J.P. Dworkin, L.A. Adelman, T. Ajluni, A.V. Andronikov, J.C. Aponte, A.E. Bartels, E. Beshore, E.B. Bierhaus, J.R. Brucato, B.H. Bryan, A.S. Burton, M.P. Callahan, S.L. Castro-Wallace, B.C. Clark, S.J. Clemett, H.C. Connolly Jr., W.E. Cutlip, S.M. Daly, V.E. Elliott, J.E. Elsila, H.L. Enos, D.F. Everett, I.A. Franchi, D.P. Glavin, H.V. Graham, J.E. Hendershot, J.W. Harris, S.L. Hill, A.R. Hildebrand, G.O. Jayne, R.W. Jenkins Jr., K.S. Johnson, J.S. Kirsch, D.S. Lauretta, A.S. Lewis, J.J. Loiacono, C.C. Lorentson, J.R. Marshall, M.G. Martin, L.L. Matthias, H.L. McLain, S.R. Messenger, R.G. Mink, J.L. Moore, K. Nakamura-Messenger, J.A. Nuth III, C.V. Owens, C.L. Parish, B.D. Perkins, M.S. Pryzby, C.A. Reigle, K. Righter, B. Rizk, J.F. Russell, S.A. Sandford, J.P. Schepis, J. Songer, M.F. Sovinski, S.W. Stahl, K. Thomas-Keprta, J.M. Vellinga, M.S. Walker, OSIRIS-REx contamination control strategy and implementation, *Space Sci. Rev.* 214 (2018) 19, <https://doi.org/10.1007/s11214-017-0439-4>.
- [8] P.R. Christensen, V.E. Hamilton, G.L. Mehall, D. Pelham, W. O'Donnell, S. Anwar, H. Bowles, S. Chase, J. Fahlgren, Z. Farkas, T. Fisher, O. James, I. Kubik, I. Lazbin, M. Miner, M. Rassas, L. Schulze, K. Shamordola, T. Tourville, G. West, R. Woodward, D. Lauretta, The OSIRIS-REx thermal emission spectrometer (OTES) instrument, *Space Sci. Rev.* 214 (2018) 39 article id. 87.
- [9] M.G. Daly, O.S. Barnouin, C. Dickinson, J. Seabrook, C.L. Johnson, G. Cunningham, T. Haltigin, D. Gaudreau, C. Brunet, I. Aslam, A. Taylor, E.B. Bierhaus, W. Boynton, M. Nolan, D.S. Lauretta, The OSIRIS-REx laser altimeter (OLA) investigation and instrument, *Space Sci. Rev.* 212 (2017) 899–924.
- [10] R.A. Masterson, M. Chodas, L. Bayley, B. Allen, J. Hong, P. Biswas, C. McMenamin, K. Stout, E. Bokhour, H. Bralower, D. Carte, S. Chen, M. Jones, S. Kissel, F. Schmidt, M. Smith, G. Sondecker, L.F. Lim, D.S. Lauretta, J.E. Grindlay, R.P. Binzel, Regolith X-ray imaging spectrometer (REXIS) aboard the OSIRIS-REx asteroid sample return mission, *Space Sci. Rev.* 214 (2018) 26 article id. 48.
- [11] D.C. Reuter, A.A. Simon, J. Hair, A. Lunsford, S. Manthripragada, V. Bly, B. Bos, C. Brambora, E. Caldwell, G. Casto, Z. Dolch, P. Finneran, D. Jennings, M. Jhabvala, E. Matson, M. McLelland, W. Roher, T. Sullivan, E. Weigle, Y. Wen, D. Wilson, D.S. Lauretta, The OSIRIS-REx visible and InfraRed spectrometer (OVIRS): spectral maps of the asteroid Benu, *Space Sci. Rev.* 214 (2018) 22 article id. 54.
- [12] B. Rizk, C. Drouet d'Aubigny, D. Golish, C. Fellows, C. Merrill, P. Smith, M.S. Walker, J.E. Hendershot, J. Hancock, S.H. Bailey, D.N. DellaGiustina, D.S. Lauretta, R. Tanner, M. Williams, K. Harshman, M. Fitzgibbon, W. Verts, J. Chen, T. Connors, D. Hamara, A. Dowd, A. Lowman, M. Dubin, R. Burt, M. Whiteley, M. Watson, T. McMahon, M. Ward, D. Booher, M. Read, B. Williams, M. Hunten, E. Little, T. Saltzman, D. Alfred, S. O'Dougherty, M. Walthall, K. Kenagy, S. Peterson, B. Crowther, M.L. Perry, C. See, S. Selznick, C. Sauve, M. Beiser, W. Black, R.N. Pfisterer, A. Lancaster, S. Oliver, C. Oquest, D. Crowley, C. Morgan, C. Castle, R. Dominguez, M. Sullivan, OCAMS: the OSIRIS-REx camera suite, *Space Sci. Rev.* 214 (2018) 26.
- [13] E.B. Bierhaus, B.C. Clark, J.W. Harris, K.S. Payne, R.D. Dubisher, D.W. Wurts, R.A. Hund, R.M. Kuhns, T.M. Linn, J.L. Wood, A.J. May, J.P. Dworkin, E. Beshore, D.S. Lauretta, The OSIRIS-REx Team, The OSIRIS-REx spacecraft and the touch-and-go sample acquisition mechanism (TAGSAM), *Space Sci. Rev.* 214 (2018) 107.
- [14] D.E. Brownlee, P. Tsou, J.D. Anderson, M.S. Hanner, R.L. Newburn, Z. Sekanina, B.C. Clark, F. Hörz, M.E. Zolensky, J. Kissel, J.A.M. McDonnell, S.A. Sandford, A. J. Tuzzolino, STARDUST: comet and interstellar dust sample return mission, *J. Geophys. Res.* 108 (8111) (2003) 1–1–1–15.

- [15] P. Tsou, D.E. Brownlee, S.A. Sandford, F. Hörz, M.E. Zolensky, Wild 2 and interstellar sample collection and Earth return, *J. Geophys. Res.* 108 (8113) (2003) 3-1–3-21.
- [16] B.J. Bos, M.A. Ravine, M. Caplinger, J.A. Schaffner, J.V. Ladewig, R.D. Olds, C.D. Norman, et al., Touch and Go Camera System (TAGCAMS) for the OSIRIS-REx asteroid sample return mission, *Space Sci. Rev.* 214 (2018) 37.
- [17] H.K. Tran, C.E. Johnson, D.J. Rasky, F.C.L. Hui, M.-T. Hsu, Y.K. Chen, Phenolic impregnated Carbon ablators (PICA) for discovery class missions, 31st Thermophysics Conference, AIAA Meeting Papers on Discovery, June 1996, <https://doi.org/10.2514/6.1996-1911> New Orleans, Louisiana, A9636374, AIAA Paper 96-1911.
- [18] B. Rizk, C. Drouet d'Aubigny, C.W. Hergenrother, B.J. Bos, D.R. Golish, R. Malhotra, D.S. Lauretta, J. Butt, J. Patel, M. Fitzgibbon, C. May, E.B. Bierhaus, S. Freund, M. Fisher, S. Cambioni, C.A. Bennett, S.S. Balram-Knutson, K. Harshman, D.N. DellaGiustina, P. Antreasian, J. Leonard, R. Mink, A. Calloway, A.E. Bartels, H. Enos, W.V. Boynton, M.C. Nolan, M. Moreau, OSIRIS-REx low-velocity particles during outbound cruise, *Adv. Space Res.* (2018), <https://doi.org/10.1016/j.asr.2018.08.020>.
- [19] B. Schläppi, K. Altwegg, H. Balsiger, M. Hässig, A. Jäckel, P. Wurz, B. Biethe, M. Rubin, S.A. Fuselier, J.J. Berthelier, J. De Keyser, H. Rème, U. Mall, Influence of spacecraft outgassing on the exploration of tenuous atmospheres with in situ mass spectrometry, *J. Geophys. Res. Space Phys.* 115 (A12) (2010), <https://doi.org/10.1029/2010JA015734>.
- [20] E.L. Andreas, New estimates for the sublimation rate for ice on the Moon, *Icarus* 186 (2007) 24–30, <https://doi.org/10.1016/j.icarus.2006.08.024>.
- [21] S.A. Sandford, L.J. Allamandola, The condensation and vaporization behavior of H<sub>2</sub>O:CO ices and implications for interstellar grains and cometary behavior, *Icarus* 76 (1988) 201–224.
- [22] D.M. Hudgins, S.A. Sandford, L.J. Allamandola, A.G.G.M. Tielens, Mid- and far-infrared spectroscopy of ices: optical constants and integrated absorbances, *Astrophys. J. Suppl.* 86 (1993) 713–870.
- [23] R.M. Mastrapa, S.A. Sandford, T.L. Roush, D.P. Cruikshank, C.M. Dalle Ore, Optical constants of amorphous and crystalline H<sub>2</sub>O-ice: 2.5–22 μm (4000–455 cm<sup>-1</sup>) – optical constants of H<sub>2</sub>O-ice, *Astrophys. J.* 710 (2009) 1347–1356.
- [24] S.A. Sandford, L.J. Allamandola, The physical and infrared spectral properties of CO<sub>2</sub> in astrophysical ice analogs, *Astrophys. J.* 355 (1990) 357–372.
- [25] D.W. White, R.M.E. Mastrapa, S.A. Sandford, Laboratory spectra of CO<sub>2</sub> vibrational modes in planetary ice analogs, *Icarus* 221 (2012) 1032–1042.
- [26] B. Rowland, M. Fisher, J.P. Devlin, Probing icy surfaces with the dangling-OH-mode absorption: large ice clusters and microporous amorphous ice, *J. Chem. Phys.* 95 (1991) 1378–1384.
- [27] S.A. Sandford, S. Bajt, S.J. Clemett, G.D. Cody, G. Cooper, B.T. DeGregorio, V. De Vera, J.P. Dworkin, J.E. Elsila, G.J. Flynn, D.P. Glavin, A. Lanzirrotti, T. Limero, M.P. Martin, C.J. Snead, M.K. Spencer, T. Stephan, A. Westphal, S. Wirick, R.N. Zare, M.E. Zolensky, Assessment and control of organic and other contaminants associated with the Stardust sample return from Comet 81P/Wild 2, *Meteorit. Planet. Sci.* 45 (2010) 406–433.